Mausam, (1989), **40**, 3, 243-246

551.501.776 : 551.509.327

Estimation of cloud microstructural parameters from satellite imagery : A Markov random field approach

SUJIT BASU, M. MOHAN and VIJAY K. AGARWAL

Meteorology and Oceanography Division, Space Applications Centre, Ahmedabad

(*Received 22 July 1988*)

सार — मेघ दृश्य की विभिन्न दिशाओं में गुच्छ निर्माण नियंत्रक सूक्ष्म संरचनीय प्राचलों के आकलन की ढूंढ की गई। मेघ दृश्य को मार्कोव यादृच्छिक क्षेत्र के रूप में दर्शाया गया है और प्राचलों का अनुमान अधिकतम संभावित तकनीक द्वारा लगाया गया है। प्रत्येक दृश्य के तदनुरूप एक प्रतिनियुक्त प्रतिबिम्ब मोन्टेकार्लो विधि द्वारा उत्पन्न होता है। नोआ (NOAA) और इनसैट (INSAT) मेघ प्रतिबिम्बों के विश्लेषण के परिणामों को प्रस्तुत किया गया है।

ABSTRACT. Estimation of microstructural parameters controlling clustering in different directions of a cloud scene is investigated. The cloud scene is represented as a Markov random field and the parameters are estimated by a maximum likelihood technique. A surrogate image, corresponding to each scene, is generated by a Monte-Carlo procedure. Results of analysing NOAA and INSAT cloud images are presented.

1. Introduction

The main motivation for studying cloud morphology is its importance in the atmospheric radiation transport. Though several models exist (Avaste *et al*. 1974 ; Harshvardhan and Weinman 1982 ; Naber and Weinman 1984; Welch and Weilicki 1984) for describing radiative transfer in three dimensionally non-uniform cloud layers, they are all far away from any realistic situation. This is largely because it is still a very difficult task to quantitatively characterise real cloud fields to make modelling very efficient. The methods widely used such as the 2D-FFT (2-dimensional Fourier Transform), spatial coherence (Rosenfeld and Kak 1976; Coakley and Bretherton 1982; Logan *et al.* 1983; Mohan *et al.* 1988) can although give a lot of information about the gross properties of clouds in an image, are inadequate in detecting their microstructural features. But a knowledge of the microstructural features of clouds or, in other words, the fine details of the cloud structure in the smaller space scales is quite important since it very often serves to distinguish different types of clouds from one another.

In this paper, we demonstrate a method for deriving a set of parameters from a cloud image which would represent the microstructural features of clouds. Our method is based on modelling a cloud image by a two dimensional random Markovian field. Together with the 2D-FFT we believe that this scheme will be able to provide more complete quantitative characteristics of cloud fields (Garand and Weinman 1986). It is obvious that the lack of knowledge of the cloud microphysical processes precludes any possibility of detailed physical analysis of cloud images. The only option available is a statistical representation of satellite images of cloud fields. Such images can reasonably well be represented by 2-dimensional Markov random fields (Cross and Jain 1983; Garand and Weinman 1986). In a two dimensional Markovian field, the probability of any pixel to have a certain grey level depends only on the grey level distribution of its neighbours. The parameters we derive express the strength of clustering of pixels in the vertical, horizontal and the two diagonal directions. They can in fact be very efficient signatures of the microstructural features of clouds. For a given cloud image, these parameters are estimated by randomly picking up pixels and relating their grey values to their neighbours in the four directions using a standard maximum likelihood technique. The reasonableness of our assumption is decided by our ability to derive these parameters and to use them to synthesise artificial cloud images which should be statistically similar to the originals with the same texture. One should bear in mind that the sampling area should be sufficiently large to contain enough grey level variations for the textural features to show up and also, the area should be suitably homogeneous as regards the compositional structure of clouds.

The details of the parameter estimation method are outlined in Section 2. In Section 3, we describe the synthesis of artificial images for a specified set of the microstructural parameters and a histogram identical to those of the originals. In Section 4, we analyse some cloud scenes produced by NOAA-6 and INSAT-1B satellites over the Arabian Sea and the Indian Ocean. The estimated parameters for the different scenes are

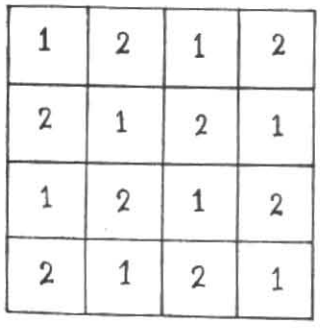

Fig. 1(a). Codings at order 1

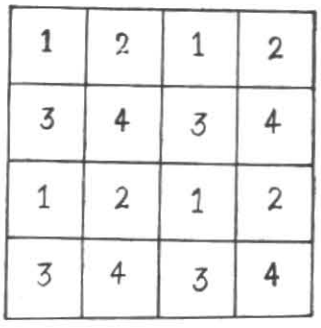

Fig. 1(b). Codings at order 2

tabulated. The original cloud scenes as well as the synthesised ones for the corresponding set of parameters are shown side by side for a comparative study. In Section 5, we discuss the results and conclusions of our work.

2. Estimation of microstructural parameters from cloud imagery

As mentioned in Sec. 1, we represent the cloud image by a two-dimensional Markovian field. However, instead of taking the whole (ordinarily, a 512×512 pixels size) image for analysis, we have chosen only 64×64 pixels size subscene, suitably homogeneous as regards cloud composition and structure. This size is also optimum from the point of view of future numerical manipulations in computer (Garand and Weinman 1986). For these reasons, the number of grey shades present in the image has been restricted to only 16.

Following Cross and Jain (1983), we assume the Markovian model to be a binomial one so that the conditional probability density is expressed as :

$$P(X_{ik}=j \mid \theta_{ik}) = ({}^{G}_{j}{}^{-1}) \ (1-\theta_{ik})^{G-1-j} \ (\theta_{ik})^{j} \qquad (1)$$

where, $P\ (X_{ik}=j|\theta_{ik})$ is the probability of the $(i,k)^{\text{th}}$ pixel to have grey level j given the configuration θ_{ik} of its neighbourhood and G denotes the number of grey levels in the image ($G=16$ in our study). By definition (Besag 1974; Cross and Jain 1983):

$$\theta_{ik} = \exp(T_{ik})/[1+\exp(T_{ik})] \qquad (2)$$

$$T_{ik} = \sum_{m=1}^{M} B(m)\, L_{ik}(m) \qquad (3)$$

In Eqn. (3), $B(1),\ldots,B(M)$ are the required microstructural parameters controlling the clustering strength in a particular direction, $M=2N+1$ is the number of parameters, N being the order of the Markov model. The directions of clustering are further implied by the constants $L(m)$. Thus, by definition $L_{ik}(1)=1$, $L_{ik}(2)$ is the sum of brightnesses of the two vertical neighbours, $L_{ik}(3)$ that of the two horizontal neighbours, while $L_{ik}(4)$ and $L_{ik}(5)$ are the sums of brightnesses of the pairs of diagonal neighbours in the northwest-southeast and northeast-southwest directions respectively. We have restricted ourselves to the cases of 1st and 2nd order models with three and five clustering parameters respectively. As already mentioned, $B(2)$, $B(3)$, $B(4)$ and $B(5)$ are quantitative measures of clustering strengths in the vertical, horizontal and the two diagonal directions. A relatively large positive or negative value for a particular B signifies a high degree of organization or fragmentation of the cloud elements along the corresponding direction. As regards $B(1)$, which does not belong to any particular direction, it is not an independent parameter and was empirically found to be related to the other parameters as $B(1) \simeq -(G-1)\sum_{m=2}^{M} B(m)$ (Garand and Weinman 1986). Models of higher orders lead to severe complexity and convergence problems in numerical calculations without contributing significantly to the cloud classification problem. The definition of neighbourhood as employed here meets with difficulty while considering the pixels lying at the four boundaries of the image. To avoid this, the image has been considered to be laterally cyclic.

For estimating the clustering parameters $B(m)$ we adopt the straight forward maximization of the logarithm of the likelihood function, *i.e.*, of :

$$L(X) = \sum_{X} \ln [P(X_{ik}=j \mid \theta_{ik})] \qquad (4)$$

where X on the R.H.S. denotes that the sum is to be performed over all pixels of a particular coding chosen in such a way that the terms of the sum are independent of one another. Thus the scene is broken up into several codings. The number of possible codings depends on the model. Figs. 1 (a) & 1 (b) represent the codings at orders 1 and 2. It is obvious that the pixels belonging to a particular coding are independent since no pixel is neighbour of any other in the same coding.

Hence, we will have two different likelihood functions at order 1 and four at order 2. Accordingly, we have two different estimates of the three parameters at order 1 and four different estimates at order 2. If the estimates are reasonably close, they have to be averaged. If they are not close, the result becomes a non-reliable one, in the sense that the Markovian model does not faithfully represent the real image. Thus, the whole problem boils down to finding the zeroes of the derivatives of $L(X)$ with respect to the individual clustering parameters $B(m)$. The roots are found by a generalised Newtonian iteration (Conte and De Boor 1980) :

$$B^{k+1} = B^{k} - J^{-1} F^{k} \qquad (5)$$

where, k is iteration number, B is the $M\times1$ column vector and F is the $M\times1$ vector of derivatives :

$$F(m) = \frac{\partial L}{\partial B(m)} = \sum_{X} \frac{L_{ik}(m)\,\{j+(j-G+1)\exp(T_{ik})\}}{\{1+\exp(T_{ik})\}} \qquad (6)$$

and J is the $M \times M$ Jacobian :

$$J(m,n) = \frac{\partial^2 L}{\partial B(m)\,\partial B(n)} = \sum_{X} \frac{L_{ik}(m)\,L_{ik}(n)\,(1-G)\exp(T_{ik})}{\{1+\exp(T_{ik})\}^2} \qquad (7)$$

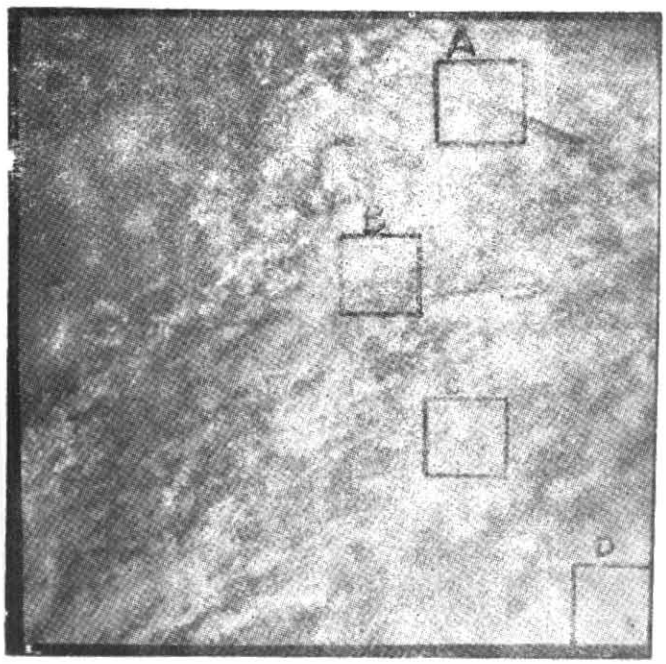

Fig. 2. NOAA-6 image of cloud over Arabian Sea with the scenes A to D marked. These scenes are each of size 64×64 pixels

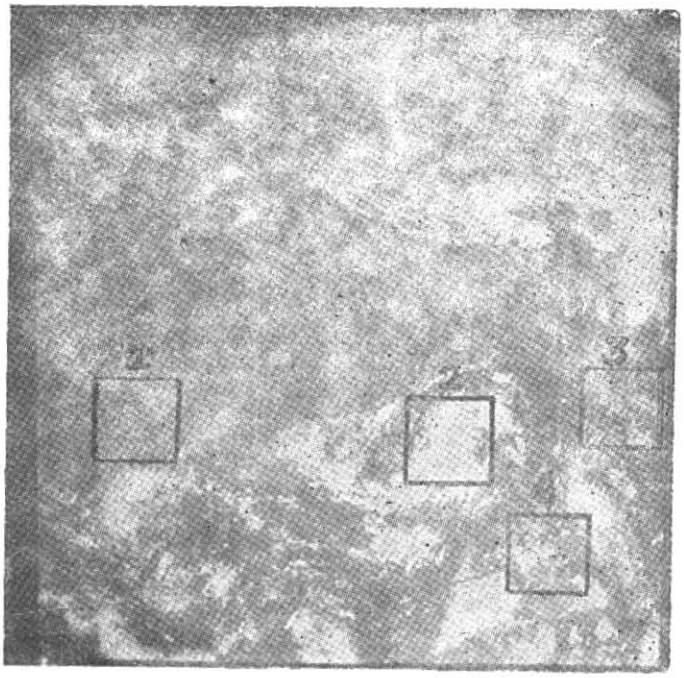

Fig. 3. INSAT-1B image of cloud over Indian Ocean with the scenes 1 to 4 marked having the same size

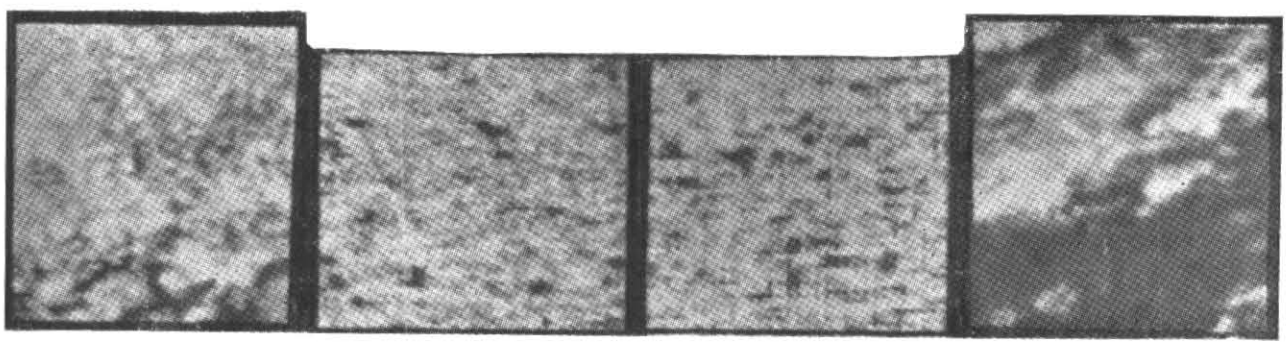

Fig. 4 (a). Enlarged and enhanced version of scene A of Fig. 2

Fig. 4(b). Surrogate image of 4(a) in first order

Fig. 4(c). Surrogate image of 4(a) in second order

Fig. 5(a). Scene B

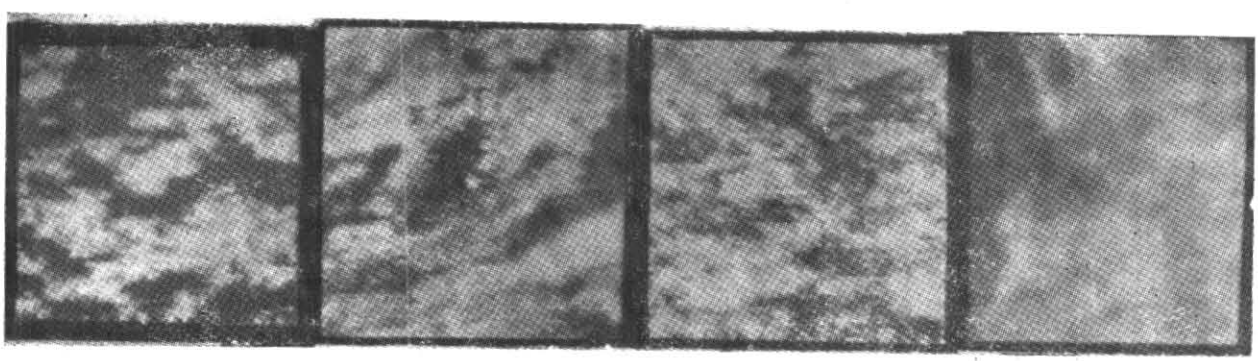

Fig. 5(b). Surrogate of scene B in first order

Figs. 6(a & b). Scene C and its surrogate in first order

Fig. 7 (a). Scene D

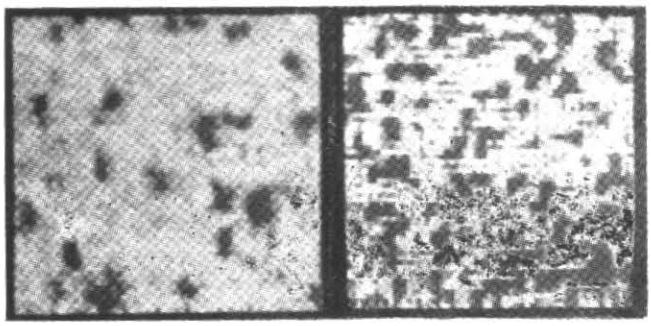

Figs. 7(b & c). Surrogates of scene D in first and second order respectively

Figs. 8(a). Enlarged and enhanced version of scene 1 of Fig. 3

Figs. 8(b). Surrogate image of scene 1 in second order

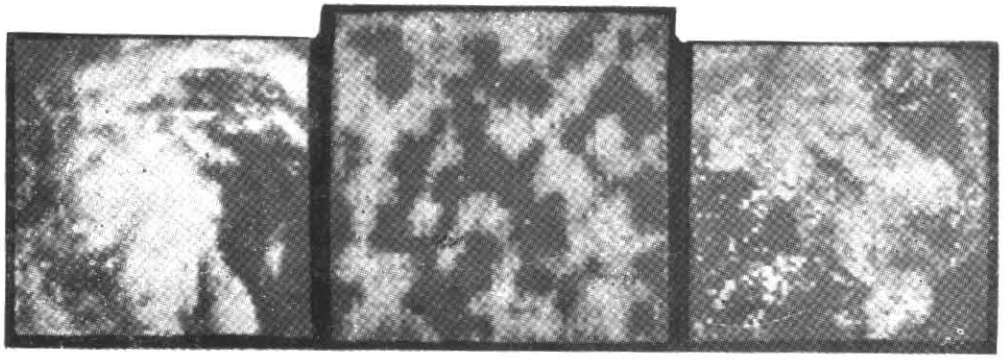

Figs. 9(a & b). Scene 2 and its second order surrogate

Fig. 10(a). Scene 3

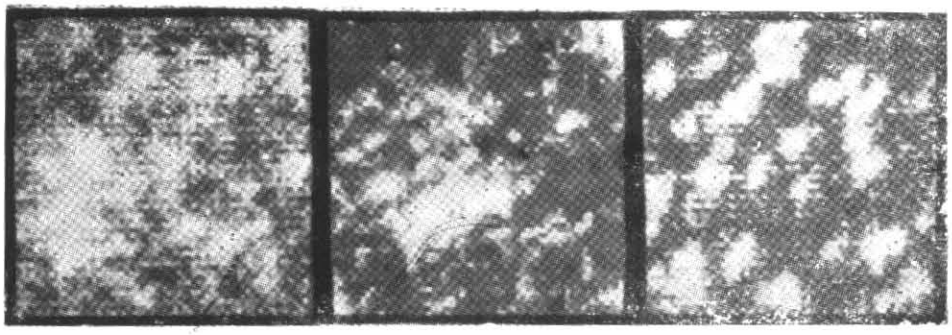

Fig. 10(b). Second order surrogate of scene 3

Figs. 11 (a & b). Scene 4 and its second order surrogate

TABLE 1

Results of first order calculation for NOAA image

Scene	Microstructural parameters		
	$B(1)$	$B(2)$	$B(3)$
A	—2.426	.043	.123
As	—2.080	.036	.102
B	—2.983	.057	.162
Bs	—2.831	.049	.149
C	—2.457	.053	.115
Cs	—2.317	.051	.104
D	—2.452	.098	.063
Ds	—2.614	.104	.064

To avoid numerical instability in inversion of a matrix we have replaced Eqn. (5) by an equivalent one :

$$J(\triangle B)^k = -F^k \tag{8}$$

where, $(\triangle B)^k = B^{k+1} - B^k$. Starting with initial guess $B(m)=0$, $m=1, \ldots, M$ Eqn. (8) was iterated to find the $(\triangle B)^k$s by a standard linear equation solver by Gaussian elimination.

Convergence was very fast, requiring typically five to six iterations in all the cases studied by us.

3. Synthesis of image with derived parameters

Starting with a white noise image having the same histogram as the original one, it is possible to synthesise an artificial image with the same (or as closely approximated as possible) set of parameters. We call this a surrogate image and it will be statistically similar to the original one as regards the textural details. The generation of the surrogate image is achieved through a process of switching of randomly picked pairs of pixels belonging to the same coding each time. This switching of pixels has to be done sufficiently large number of times till the parameters are brought as close to the original ones as possible. Because of the statistically random nature of this switching process, it is next to impossible to achieve exact coincidence of the parameters. The degree of closeness between them is an indirect measure of applicability of the Markov model. However, in all the cases studied here, the agreement was reasonably good.

If X represents the image before switching and Y that after, then the criterion for taking the decision of switching is the ratio $P(Y)/P(X) = R$. If $R \geqslant 1$, the pixels picked at random (but belonging to the same coding) are switched. If $R<1$, then R is compared with the output of a uniform pseudo-random number generator in (0, 1) and if R is found to be greater than this output, then the switching is done. This technique was devised by Metropolis *et al.* (1953). With the above mentioned restriction of choosing the two pixels from a particular coding, the expression for R becomes (Garand and Weinman 1986) :

$$R = \exp(T_2 - T_1)^{x_1 - x_2} \tag{9}$$

where, x_1 and x_2 are grey levels of the two pixels. One iteration consists of S^2 attempted exchanges with S^2 being the total number of pixels (4096, in our case). After a few iterations, the total number of change becomes nearly constant, signifying that the Markov process has attained stationarity. By trial and error, we have found that about thirty iterations are sufficient for all the scenes analysed by us. At this stage, we estimated the parameters of the resulting image by the procedure outlined in Sec. 2. As will be shown in Sec. 4, in all cases encountered by us, the parameters of the surrogate images were reasonably close to those of the real ones, thus proving the correctness of parameter estimation. Also the synthesised images look texturally similar, of course, in a statistical sense, to the original ones.

4. Analysis of the NOAA and INSAT cloud images

Fig. 2 is a NOAA-6 digital infrared image of a cloudy scene taken on 20 November 1980, over the Arabian Sea. We have chosen four distinct scenes from this image as indicated by the square boxes each of size 64×64 pixels and subjected them to the Markovian analysis. These scenes are chosen on the basis of having clouds with more or less uniform distribution and morphology. In a similar manner, we have chosen four scenes from an INSAT-1B digital visible cloud image (Fig.3) over the Indian Ocean taken on 10 November 1984. We have represented the full range of grey level in each scene in terms of 16 discrete shades, from 0 to 15. It has been found that the textural details of clouds represented by the microstructural parameters are retained even with 16 grey levels. Moreover, by keeping the range of grey level same for all images, it becomes easy to compare different cloud scenes quantitatively. On the other hand, if we use the full ranges of grey levels of the original scenes which are usually very large the number of possible neighbourhood configurations of each pixel becomes extremely large that cannot be well represented statistically. Besides, that will also lead to numerical difficulties in the computations because of the binomial probability distribution used. But for better contrast these images are presented in their enlarged versions [Figs. 4 (a) to 7 (a) for NOAA and Figs. 8 (a) to 11 (a) for INSAT] in an enhanced form. Due to this, the appearances of the scenes in the original images and their reproduced versions are slightly different, notably in the case of scene D of Fig. 2.

We have carried out the first order Markovian analysis for the NOAA scenes and second order analysis for the INSAT scenes and two of the NOAA scenes. After the microstructural parameters were retrieved from these scenes, a surrogate image in each case was also synthesised [(Figs. 4 (b) to 7 (b), 4 (c) and 7 (c) for NOAA and Figs. 8(b) to 11(b) for INSAT]. The parameters of the original as well as the surrogate images are displayed in Tables 1 to 3 . In these tables, the suffix 'S' after a scene index denotes the surrogate version of the corresponding original.

Table 1 gives the results of the first order calculations in which $B(2)$ and $B(3)$ represent the clustering strength in the vertical and the horizontal directions respectively as mentioned in Sec. 2. It can be seen that the values of

TABLE 2

Results of second order calculations for the scenes A and D of NOAA image

Scene	Microstructural parameters				
	B(1)	*B*(2)	*B*(3)	*B*(4)	*B*(5)
A	—2.305	.089	.143	—.043	—.033
A_{S2}	—2.144	.080	.123	—.034	—.026
D	—2.401	.137	.134	—.059	—.053
D_{S2}	—2.470	.156	.153	—.075	—.068

the parameters for the synthesised images agree reasonably well with those of the original ones. The apparent differences among the appearances of the original scenes in spite of the close values for their parameters (*e.g.*, scenes A and C of Fig. 2) can be attributed to the wide differences in their histograms.

In Table 2, we present the second order results for the two widely different scenes A and D whose first order parameters are given in Table 1. A comparison between these two tables for the first three parameters shows that the values do not agree very well. This apparent discrepancy is due to the dependence of the estimation process on the order of the model. In the first order, the diagonal clustering is completely ignored and thus, we have only two codings whereas in the second order, the diagonal clustering is explicitly taken into account and so, we have four codings. This indicates that while comparing two different cloud scenes the parameters have to be determined to the same order.

It is obvious that for more detailed information of the cloud morphology one has to prefer second order to the first order Markov model. Consequently, for the four scenes belonging to the INSAT image, we have employed only the second order calculations. These results are presented in Table 3.

In Table 3, some parameters (*e.g.*, in the diagonal directions) have been shown as negligible. This is due to the fact that the corresponding numerical values were several orders of magnitude smaller than the rest and we believe that they were very insignificant indicating the absence of any clustering in those particular directions. It is worthwhile to mention that this feature was maintained in the corresponding surrogate versions.

TABLE 3

INSAT image results

Scene	Microstructural parameters				
	B(1)	*B*(2)	*B*(3)	*B*(4)	*B*(5)
1	—2.780	.092	.086	Negligible	.036
1s	—2.672	.096	.080	Do.	.026
2	—2.630	.117	.080	—.018	Negligible
2s	—2.879	.130	.093	—.028	Do.
3	—3.183	.092	.081	.051	.058
3s	—2.936	.080	.063	.045	.040
4	—3.000	.111	.077	Negligible	.042
4s	—2.999	.113	.079	Do.	.034

5. Summary and conclusions

In this work, we have described and demonstrated the usefulness of the Markovian approach in the quantification of the cloud microstructural properties. We believe this to be an important step in the quantitative classification of clouds into different types. This method is very effective when a large number of cloud scenes are to be analysed since, being fully computerised, it leaves no scope for subjective human errors. However, it should be borne in mind that this scheme is to be supplemented with other informations about the cloud microstructural properties ascertainable through other analyses such as 2D-FFT, clustering technique etc. Efforts have been undertaken to supplement this method with 2D-FFT. In this new scheme, we are starting with a primitive image better than the white noise one for the generation of the surrogate. This provides a better visual similarity of the surrogates to the originals. This work will be reported later.

It may be possible, in future, to study the clouds associated with the onset of monsoon by studying the time evolution of their microsturctural parameters and gain further insight into the study of monsoon. It will also be of great interest to find out any possible correlation between these parameters and the physical properties of clouds such as their albedo, emissivity, liquid water content etc so that regression relations could be found for calculating these properties in terms of microstructural parameters of the cloud considered.

References

Avaste, O.A., Mullamaa, Y.R., Nylisk, K.H. and Sulev, M. A., 1974, cited in *Heat transfer in the atmosphere,* NASA Tech. Transl. TT-F-790, 173-181.

Besag, 1974, *J. Roy. Stat. Soc.*, **B 36**, 192-326.

Coakley, J.A. and Bretherton, F.P., 1982, *J. geophys. Res.*, **87**, 4917-4932.

Conte, S.D. and De Boor, C., 1980, *Elementary Numerical Analysis*, McGraw Hill, New York, 432 pp.

Cross, G.R. and Jain, A.K., 1983, *IEEE Trans. Pattern Anal. Mach-Intell.*, PAMI-5, 25-39.

Garand, L. and Weinman, J.A., 1986, *J. Cl. Appl. Met.*, **25**, 1052-1068.

Harshvardhan and Weinman, J.A., 1982, *J. atmos. Sci.*, **38**, 431-439.

Logan, T.L., Huning, J.R. and Glackin, D.L., 1983, Cloud cover typing from environmental satellite imagery-discriminating cloud structure with FFT, Jet Propulsion Laboratory Publ.; 84-17, JPL. Pasadena.

Metropolis, N.A., Rosenbluth, A.W., Rosenbluth, M.N., Teller, A.H. and Teller, E., 1953, *J. Chem. Phys.*, **21**, 1087-1091.

Mohan, M., Bhaduri, L. and Agarwal, V.K., 1988, *Proc. Indian Acad. Sci.* (Earth Planet Sci.), **97**, 159-171.

Naber, P.S. and Weinman, J.A., 1984, *J. geophys. Res.*, **89**, 1249-1257.

Rosenfeld, A. and Kak, A.C., 1976, *Digital Picture Processing*, Academic Press. Inc., New York, 457 pp.

Welch, R.M. and Weilicki, B.A., 1984, *J. atmos. Sci.*, **41**, 3085-3103.